Synthesis, structures, electrochemical and quantum chemical investigations of Ni(II) and Cu(II) complexes with a tetradentate Schiff base derived from 1-(2-thienyl)-1,3-butanedione

Guillermo Ahumada, Jocelyn Oyarce, Thierry Roisnel, Samia Kahlal, Maria Angelica del Valle, David Carrillo, Jean-Yves Saillard, Jean-René Hamon, Carolina Manzur

Synthesis, structures, electrochemical and quantum chemical investigations of Ni(II) and Cu(II) complexes with a tetradentate Schiff base derived from 1-(2-thienyl)-1,3-butanedione[†,‡]

Guillermo Ahumada,[a,b] Jocelyn Oyarce,[a] Thierry Roisnel,[b] Samia Kahlal,[b] María Angélica del Valle,[c] David Carrillo,[a] Jean-Yves Saillard,[b] Jean-René Hamon*[b] and Carolina Manzur*[a]

a *Laboratorio de Química Inorgánica, Instituto de Química, Facultad de Ciencias, Pontificia Universidad Católica de Valparaíso, Campus Curauma, Avenida Universidad 330, Valparaíso, Chile. E-mail: cecilia.manzur@pucv.cl*

b *Univ Rennes, CNRS, ISCR (Institut des Sciences Chimiques de Rennes) – UMR 6226, F-35000 Rennes, France. E-mail: jean-rene.hamon@univ-rennes1.fr*

c *Laboratorio de Electroquímica de Polímeros (LEP), Pontificia Universidad Católica de Chile, Vicuña Mackenna 4860, 7820436 Macul, Santiago, Chile*

† **Electronic supplementary information (ESI) available.** CCDC 1852010 and 1852011 (**3** and **4**). For ESI and crystallographic data in CIF or other electronic format see DOI:

‡ Dedicated to the memory of our esteemed colleague Prof. Jean-Yves pivan (ENSC-Rennes)

Abstract

Double condensation of the newly prepared 1-(2-thienyl)-1,3-butanedione with ethylenediamine lead to the formation of the novel symmetrical Schiff base proligand bearing two potentially electropolymerizable 2-thienyl groups. Both organic species were obtained in 55 and 80% yields, respectively. They exist as their respective keto-enol and enaminone tautomeric forms that were computed to be more stable by 8.6 and 30.3 kcal/mol than their β-diketone and keto-imine isomers. The corresponding Ni(II) and Cu(II) complexes featuring a N_2O_2-tetradentate Schiff base ligand were readily synthesized upon reaction of the diprotic Schiff base precursor with the appropriate hydrated metal acetates, and isolated as neutral, air and thermally stable solids in excellent yields (84 and 90%). The four compounds were characterized using various analytical and spectroscopic methods, and by X-ray diffraction study for the two coordination complexes. Both Ni(II) and Cu(II) metal ions are four-coordinated and adopt a perfect square planar environment (τ_4 value of 0.036 and 0.025) with two nitrogen and two oxygen atoms as donors. Both complexes were analyzed by cyclic voltammetry experiments showing a decrease of the current response per cycle, indicating the formation of oligomeric units. This was verified by their doping/undoping responses. Optimized geometries of the four compounds as well as the electronic structures of the two Ni(II) and Cu(II) complexes and their respective cations have been analysed through DFT calculations, allowing providing a consistent view of their structure and properties. TDDFT calculations have been used to interpret the major features of the UV-vis. spectra.

Introduction

Almost 130 years ago, Combes reported the first and simplest symmetrical Schiff base derivative resulting from condensation of acetylacetone with ethylenediamine in the 2:1 molar ratio, as well as its corresponding copper(II) complex obtained upon reaction with cupric acetate.[1] Since then, the preparation and study of the class of acyclic N_2O_2 tetradentate based Schiff base ligands and their complexes greatly participated to the booming of a very fertile and dynamic research field in coordination chemistry.[2-4] The versatility of Schiff base ligands arises from their structural and electronic variations, achieved by varying the stereo-electronic nature of the substituents incorporated on their skeletons via the β-diketone starting materials.[5] Those easily synthetized and easily tunable dicarbonyl building blocks, presenting a keto-enol tautomerism,[6-8] are readily tailored to bring about donor, acceptor, polymerizable, or electroactive groups at the three carbon atoms constituting the propane-1,3-dione skeleton.[7-14] β-diketones containing a thiophene group are of particular interest because they can be used as starting materials for the construction of Schiff base derivatives and metal complexes tagged with electroactive thiophene moieties, thus allowing electrochemical polymerization to conveniently enable the direct preparation of an insoluble polymeric coating on the surface of the electrode.[15-17]

In this context, we have recently disclosed the generation and characterization of a polythienyl-containing β-diketonate copper(II) compound and its deposition on an electrode, upon electropolymerization of the [Cu(II)-bis-{1-(2-thienyl)-3-(3-thienyl)propane-1,3-dionato}] complex using potentiodynamic method.[18] By contrast, no deposits of polymeric species on the electrode surface could be observed upon changing the thiophen-3-yl group for the more electron-withdrawing 4-fluorophenyl unit.[19] A similar observation was made with a series of cobalt(II), nickel(II) and copper(II) complexes of a fluorinated Schiff base ligand formally resulting from the condensation of 2-thenoyltrifluoroacetone (TTA) with 1,2-diaminoethane; cyclic voltammograms of these complexes displayed indeed oxidation waves, but none of them formed polymer films upon repeated cycling.[20] Those experiments clearly demonstrate that the electronics play an important role in the final outcome of the electropolymerization process. Therefore, pursuing along this line, we thought that such electropolymerization could be applied to first raw transition metal complexes with the symmetrically-substituted electron-rich Schiff bases **2** obtained by double condensation of ethylenediamine with the known 2-thenoylacetone **1**, that mainly exists as its keto-enol tautomer (*Z*)-4-Hydroxy-4-(2-thienyl)-3-buten-2-one[10,11] (see formulas in Scheme 1).

Herein, we report on a new template synthesis of **1**, the preparation of the Schiff base proligand **2** and its reactions with the appropriate metal(II) acetate salt in order to synthesize the N_2O_2-tetradentate Schiff base complexes of Ni(II) **3** and Cu(II) **4** (see formulas in Schemes 2). All the compounds were fully characterized by analytical and spectroscopic techniques. Both complexes **3** and **4** were authenticated by single crystal X-ray diffraction analysis. In addition, the geometries and electronic properties of **1**-**4** were investigated by density functional (DFT) and time-dependent DFT (TD-DFT) calculation. Electrochemical study of complexes **3**-**4** was carried out by cyclic voltammetry, showing the formation of low conductivity oligomeric units that possess a fully reversible charge response.

Results and Discussion

Synthesis and characterization

The asymmetric β-diketone **1** was prepared in a two-step procedure (see Scheme 1) and isolated in 55% yield as a white solid that decomposes above 50 °C. 2- acetylthiophene was first treated with potassium *tert*-butoxide and ethyl acetate at ambient temperature,[21] followed by a templated purification procedure of the formed β-diketone using copper(II) acetate (see Experimental). In a recent work, Prabhu *et al.*[11] used NaH (60% suspension in paraffin oil) as the base initiator in THF at 0 °C, and obtained **1** as a yellow liquid (no yield communicated). Compound **1** has also been synthetized by the LDA-mediated reaction of acetone with 2-thiophenecarbonyl chloride in THF at -78 °C and isolated in 34% yield as a yellowish oil.[10] Although we prepared compound **1** as a white solid whose high purity was established by combustion analysis, its IR, ^{1}H and ^{13}C NMR spectral data (see Experimental) fully agree with the reported keto-enol structure (*Z*)-4-Hydroxy-4-(2-thienyl)-3-buten-2-one elucidated by 2D NMR method.[10] Only this isomer is found in solution and in the solid-state. Note that in the case of the NaH-mediated reaction, the isolated product is a 85/15 keto-enol/diketone tautomeric mixture.[11]

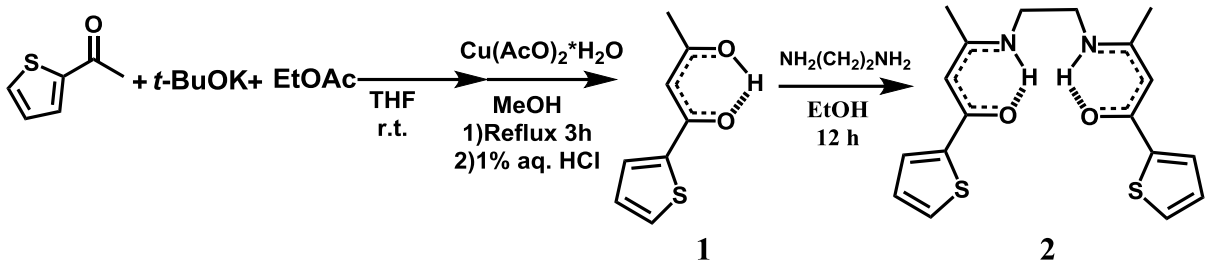

Scheme 1. Synthesis of the β-diketone **1** (keto-enol tautomer) and its derivatized Schiff base **2**.

The symmetrically-substituted Schiff base **2** was readily synthesized by condensation of 1,2-diaminoethane with 2 equivalents of **1** in dry ethanol for 18 h at ambient temperature (Scheme 1). Compound **2** was isolated in 80% yield as an air and moisture sensitive yellow powder. Like **1**, it is better to store **2** neat under a nitrogen atmosphere at low temperature (-30 °C). All attempts to increase the yield or to reduce the reaction time by either heating or using catalyst such as acetic acid lead to decomposition of the final product. Schiff base **2** is highly soluble in common organic solvents (CH_2Cl_2, THF, Et_2O, *n*-hexane).

Complexes **3** and **4** were facilely obtained by reacting the Schiff base proligand **2** with either hydrated nickel or copper acetate salt in methanol at ambient temperature for 4 h (Scheme 2). The two compounds were isolated as air and thermally stable, and moisture insensitive on storage under ordinary conditions, light brown **3** and green **4** solids in excellent yields of 84 and 90%, respectively. They show good solubility in polar organic solvents such as dichloromethane, tetrahydrofuran and methanol, but are insoluble in diethyl ether and hydrocarbon solvents.

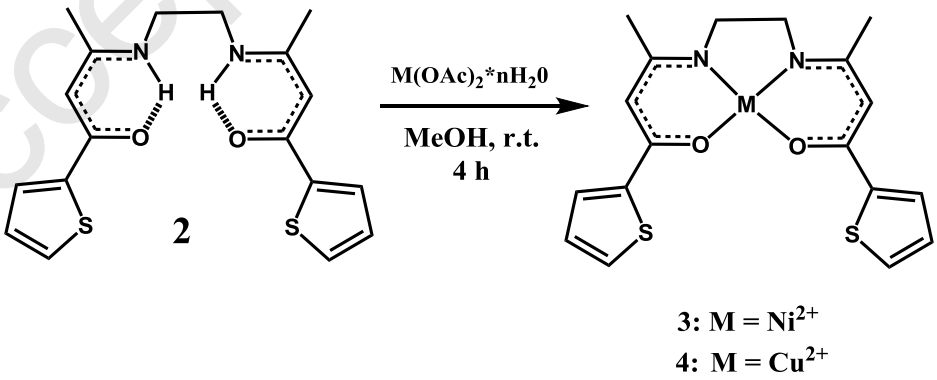

Scheme 2. Synthesis of the symmetrically-substituted Schiff base complexes **3** and **4**.

Elemental analyses (CHNS) of all the compounds (**1**-**4**) showed that the calculated and found values for carbon, hydrogen, nitrogen, and sulfur are in good agreement with each other, which established that the four species are amply pure in bulk. The proposed structures are based on spectroscopic characteristics (FT-IR, UV-vis., ^{1}H and ^{13}C NMR of diamagnetic **1**-**3**), and single crystal X-ray diffraction studies of both complexes **3** and **4**. Moreover, the structure of the paramagnetic Cu(II) derivative **4**, was confirmed by HRMS ESI^{+}, where the sodium aggregate appeared at m/z = 444.00 (see Experimental).

The solid-state FT-IR spectrum of the β-diketone **1** exhibited a strong band at 3460 cm^{-1} assigned to the ν(O-H) stretching mode, and a series of three strong to medium intensity band at 1615, 1519 and 1413 cm^{-1} attributed to the C···O and C···C stretching vibrations. The lack of ν(C=O) absorption observed at 1721 cm^{-1} for a neat liquid sample of **1**,[11] clearly suggests that the presently prepared **1** does only exist as its keto-enol tautomeric form in the solid-state. In the spectrum of the free Schiff base **2**, the weak band observed at 3444 cm^{-1} is due to the ν(N–H) vibration, thus indicating that the enamine tautomer is the predominant form in the solid-state.[22] Three strong characteristic absorptions due to the [O···C···C···C···N] enaminone core are also observed at 1595, 1558 and 1529 cm^{-1}. In the spectra of complexes **3** and **4**, those bands decrease in energy by 14/7, 28/31 and 21/23 cm^{-1}, respectively, in agreement with coordination of the dianionic Schiff base ligand **2**$^{2-}$ to the Ni(II) and Cu(II) ions through the oxygen and nitrogen atoms, thus forming a six-membered heterometallacycle. Furthermore, this is confirmed by the disappearance of the ν(N-H) absorption band seen in precursor **2**. Finally, each compound showed a medium intensity band in the range 705-750 cm^{-1} assigned to the out-of-plane bending vibration mode of the C-H groups of the 2-thiophenyl unit.[23]

The ^{1}H NMR spectrum of compound **1** (Fig. S1, ESI†) showed two sharp and one broad signals at δ_{H} 2.11, 6.29 and 15.80 ppm with integral ratio 3:1:1 attributed to the methyl, methine and bridging enol protons, respectively. That of the free Schiff base **2** (Fig. S1, ESI†) presented a similar peak and integration pattern with the protons of the methyl, methine and intramolecularly hydrogen bonded amine groups showing up upfield shifted at δ_{H} 2.03, 5.56 and 11.17 ppm, respectively. Additionally, the single peak of the four magnetically equivalent protons of the ethylene linker was seen at δ_{H} 3.51 ppm. The downfield chemical shifts observed in **1** and **2** clearly suggest that both their respective enol and enaminone forms that are stabilized by intramolecular hydrogen bonding predominate in solution. Furthermore, the molecular structure of **2** was unambiguously established by 2D-HMBC ^{1}H-^{13}C NMR experiments. The

2D-spectrum (Fig. S2, ESI†) showed that the enamino carbon signal at δ_C 164.58 ppm can be correlated with the methyl, methylene and methine proton resonances, thus firmly demonstrating that the acetyl carbonyl group of **1** reacted with the amino group of 1,2-diaminoethane to form the C-N bond of the enamine fragment. By contrast, the carbonyl carbon signal at δ_C 181.28 ppm was found to only correlate with that of the methine proton. This proposed structure of **2** was later confirmed as its doubly deprotonated ligand form in the crystal structures of complexes **3** and **4** (see below). This Schiff condensation, taking place at the acetyl carbonyl carbon of **1**, sharply contrasts with the opposite situation observed with the related 2-thenoyltrifluoroacetone, where the condensation occurred at the thenoyl carbonyl carbon.[24] The crystal structure of the enol form of the fluorinated diketone starting material showed that the hydroxyl group is adjacent to the CF_3 unit.[25]

In the ^{1}H NMR spectrum of complex **3** (Fig. S1, ESI†), the signal of the amine proton vanished while those of methyl, methylene and methine groups are slightly upfield shifted, appearing at δ_H 1.96, 3.08 and 5.55 ppm, respectively. The proton-decoupled ^{13}C NMR spectral data (see Experimental for complete assignments) confirms both the proposed keto-enol and keto-enamine structures of **1** and **2**, respectively, with resonances attributed to the methine carbon nucleus observed at δ_C 96.87 and 92.61 ppm, as well as the symmetrical nature of the free Schiff base **2** and its Ni(II) complex **3** with the nine lines observed in their respective spectra (Figure S3, esi†).

Electronic absorption spectra

The UV-vis. spectra of the 2-thenoylacetone **1** (Fig. S4, ESI†), of the Schiff base proligand **2** and its related metal(II) complexes **3** and **4** (Fig. 1) were recorded in dichloromethane solutions at 20 °C. Absorption spectral data are gathered in Table 1. In the spectrum of proligand **2**, the observed maximum absorptions at 282 nm, and 362 nm are due to $\pi\rightarrow\pi^*$ transitions, according to the TD-DFT simulated results (see below). The peak at 257 nm has a substantial $\pi\rightarrow\sigma(CH_2CH_2)^*$ character, due to its non-planar structure (see below and Fig. S5, ESI†). TDDFT indicates also that these transitions do not exhibit any significant $n\rightarrow\pi^*$ character. Although the agreement between the experimental and simulated spectra of **3** and **4** is not as good as for **1** and **2**, $\pi\rightarrow\pi^*$ transitions were also found in the spectra of the complexes (LLCT in Table 1). The low energy band of **3** at 564 nm was not reproduced by TD-DFT and

can be tentatively assigned to a forbidden d-d transition. That at 412 nm can be indexed as of MLCT character. In the case of **4**, the two low-energy bands are found to be of LMCT nature.

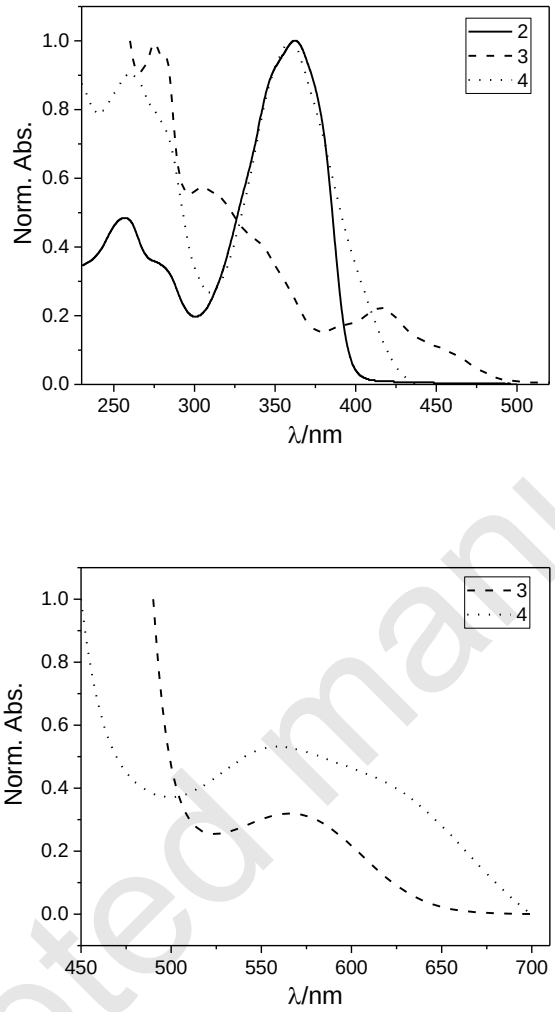

Fig. 1 UV spectra (top) and Vis spectra (bottom) of proligand **2** (solid line) and complexes **3** (dashed line) and **4** (dotted line), measured in CH_2Cl_2 solutions at 20 °C.

Table 1. Experimental and computed electronic absorption data of compounds **1**-**4**.

Compd.	λ_{max} (exp.) / nm (log ε) (CH_2Cl_2)	λ_{max} (simul.) / nm[a] (rel. absorbance) (from TD-DFT)	Major transition involved (from TD-DFT)
1	265 (4.22) 320 (4.61)	294 (8491) 337 (23433)	$\pi\rightarrow\pi^*$ $\pi\rightarrow\pi^*$
2	257 (4.19) 282 (4.04)	258 (8878) 302 (27475)	$\pi\rightarrow\sigma^*$ $\pi\rightarrow\pi^*$

	362 (4.50)	369 (39295)	π→π*
3	280 (5.26) 307 (5.30) 346 (4.99) 412 (4.88) 564 (1.82)	282 (38452) - 347 (38679) 457 (9289) -	LLCT - LLCT MLCT (HOMO-2→LUMO+1) -
4	258 (4.89) 280 (5.11) 360 (5.30) 571 (2.27)	- 314 (42114) 398 (16629) 476 (7114)	- LLCT LMCT (HOSO(β)-9→LUSO(β)) LMCT (HOSO(β)-3→LUSO(β))

[a] Spectra simulated assuming Gaussian half-height bandwidths of 3000 cm^{-1}

X-ray Crystallographic Study

Crystals of complexes **3** and **4** suitable for X-ray diffraction analysis were obtained by slow evaporation of their respective saturated ethanolic solution. A perspective view of **3** is presented in Fig. 2. The molecular structure of **4**, whose structure determination resulted in a poor resolution (R_{int} = 0.1449 and R_1 = 0.1103), is displayed in Fig. S6 (ESI†), showing the atom connectivity. Selected bond distances and angles of the first metal(II) coordination sphere of **3** and **4** are given in Table 2, while those of the Schiff base ligands of the two complexes are provided in Table S1 (ESI†). Both complexes crystallize in the monoclinic crystal system in the centrosymmetric space group $P2_1/n$ with a single molecule in the asymmetric unit. As expected, the X-ray diffraction study of **3** and **4** confirm the proposed structure of proligand **2** (see 2D NMR above), and that both complexes consist of a metal(II) ion tetracoordinated by the N_2O_2 donor set of the same dianionic Schiff base ligand symmetrically substituted with methyl and 2-thienyl groups, forming monomeric units. Both complexes are isostructural species that differ only by the nature of the M(II)-centered metal ion, M = Ni for **3** and Cu for **4**. The 2-thienyl rings are strongly disordered thus precluding any further discussion of their metrical parameters. We previously observed such a disorder, albeit much weaker, in structures of thiophen-containing compounds solved at low temperature.[18-20] All close intermolecular contacts correspond to van der Waals interactions.

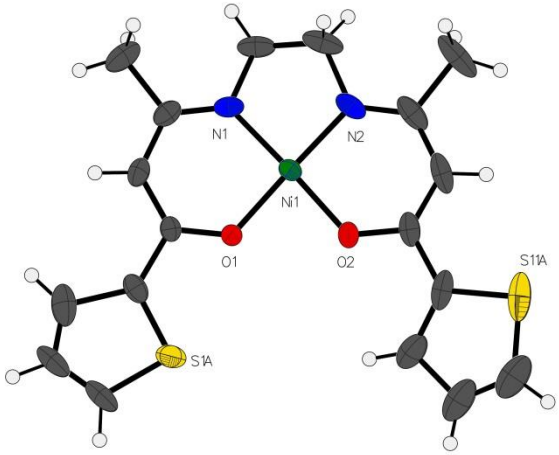

Fig. 2 Molecular structure of the Ni(II) complex **3** with a selected atom numbering scheme. Thermal ellipsoids are drawn at the 50% probability level.

Both complexes, **3** and **4**, contain a Ni(II) and a Cu(II) atom, respectively, in a four-coordinate quasi-perfect square planar geometry bonded to the four N_2O_2 donor atoms set of the tetradentate dianionic Schiff base ligand, with average Ni-O, Ni-N, Cu-O and Cu-N bond distances (Table 2) of 1.850, 1.856, 1.911 and 1.930 Å, respectively. The extent of deformation in a tetracoordinated complex can be quantified by the four-coordinate geometry τ_4 index.[26] This parameter that measures the extent of distortion between a perfect square planar geometry ($\tau_4 = 0$) and a perfect tetrahedral geometry ($\tau_4 = 1$), is obtained by the formula: $\tau_4 = [360° - (\alpha + \beta)]/141°$, α and β being the two largest bond angles of the metal coordination sphere. The Ni(II) complex **3** has a τ_4 value of 0.036 over 0.025 for the Cu(II) congener **4**. The central Ni(II) and Cu(II) atoms barely deviate from the basal plane by 0.019(1) Å and 0.024(3) Å, respectively. The angular summations of 359.97° (for **3**) and 359.90° (for **4**) are equal to the idealized value of 360° within the experimental error. Although the molecules are packed to form centrosymmetric pairs in which the metal centers are superimposed on top of each other and the nitrogens of the coordination pocket of one molecule are aligned with the oxygens of the second molecule and vice versa (Fig. S7, ESI†), there are no significant interactions in axial positions. The closest contacts are 3.4871(15) Å for Ni(1)···Ni(1)$^{\#1}$ and 3.4490(12) Å for Cu(1)···Cu(1)$^{\#1}$ (#1: 1-x,1-y,1-z). Interestingly, such M···M separations are of the same order as those we previously observed for nickel and copper complexes with unsymmetrically-substituted N_2O_2-tetradentate metallocene-containing Schiff base ligands.[27,28]

On the other hand, the atoms that constitute the two six-membered heterometallacycles [M(1)-O(1)-C(6)C(7)-C(8)-N(1)]/[M(1)-O(2)-C(16)C(17)-C(18)-N(2)] (Fig. 2) formed upon the coordination of the doubly deprotonated Schiff base **2** to the metal(II) ion, are nearly coplanar in both **3** and **4**, with rms deviations of 0.040/0.008 Å and 0.031/0.010 Å, respectively. This flatness, along with the O-C, C-C and C-N bond falling between single and double bond lengths and bond angles of sp^2 hybridized atoms (Table S1, ESI†), suggests a significant electron delocalization within the chelating rings. These two six-membered metallacycles are also almost coplanar with their respective attached 2-thienyl rings, making dihedral angles of 2.66(9)/11.90(3)° for **3** and 5.20(9)/11.85(5)° for **4**. Moreover, the five-membered metallocycle [M(1)-N(1)-C(10)-C(20)-N(2)] of both complexes **3** and **4** assumes an envelope conformation with C(10) as the flap atom (Fig. 2), deviating from the mean [N(1)-M(1)-N(2)-C(20)] plane by 0.401(7) and 0.3785(15) Å, respectively.

Table 2. Selected X-ray and corresponding DFT-optimized (in square brackets) bond distances (Å) and angles (°) for the first metal(II) coordination sphere of compound **3** and **4**.[a]

	3	**4**
Bond distances		
M(1)-O(1)	1.846(3) [1.885]	1.905(6) [1.970]
M(1)-O(2)	1.854(3) [1.881]	1.917(6) [1.966]
M(1)-N(1)	1.861(4) [1.873]	1.950(8) [1.977]
M(1)-N(2)	1.851(4) [1.879]	1.908(9) [1.976]
Bond angles		
O(1)-M(1)-N(2)	178.09(16) [178]	178.20(3) [174]
O(2)-M(1)-N(1)	176.84(14) [178]	178.20(3) [174]
O(1)-M(1)-O(2)	83.04(12) [84]	85.90(3) [89]
O(1)-M (1)-N(1)	94.52(15) [95]	93.80(3) [93]
O(2)-M(1)-N(2)	95.28(17) [95]	94.20(4) [93]
N(1)-M(1)-N(2)	87.13(19) [87]	86.00(4) [85]

[A] M = Ni, **3**; Cu, **4**.

Electrochemical studies

The electrochemical oxidation of complexes **3** and **4** was investigated by cyclic voltammetry (CV) using acetonitrile as solvent, at ambient temperature. All redox potentials are quoted versus saturated calomel electrode (SCE). CV measurements were carried out in the potential range previously established as optimal for each compound: -0.2 to 1.8 V for complex **3** and 0.1 to 1.8 V for complex **4,** respectively. Both complexes present a similar potentiodynamic behavior where two oxidation processes were found, the first one, E_1, around 1.0 V and a second one, E_2, around 1.5 V (figs. 3 and 4). The first peak is attributed to the oxidation of the metal center, whose peak of the respective reduction, when reversing the potential sweep, is observed in the first case (compound **3**) at around 1.0 V, and in the second case (compound **4**) near 0.8 V. This shows that the first redox process of **3** is electrochemically

reversible (ΔE_p < 60 mV), so that its potentials do not vary depending on the number of successive cycles, however, in the case of compound **4**, it is a quasi-reversible process (ΔE_p > 60 mV), which is manifested not only by the difference between its oxidation and reduction peak potentials, but also by the reduction potential, which moves towards less positive values depending on the number of cycles. At the same time, in both cases the currents of these peaks are decreasing, and practically disappearing in cycle 20.

The second oxidation peak is attributed to the oxidation of the thienyl moiety. In both cases, in the response of the modified electrodes a reduction process is observed around 0.0 V and it could be attributed to the *p*-doping/undoping process characteristic of modified electrodes with deposits of oligomers or conducting polymers. It is important to note that, also in this oxidation process, responsible for the formation of oligomers of chains that are lengthened by successive scans, the current is decreasing. This is attributable to the low conductivity of the deposit formed and/or to the fact that the oligomeric structure prevents the growth of the chains enough to form the polymer, reaching only oligomer levels.

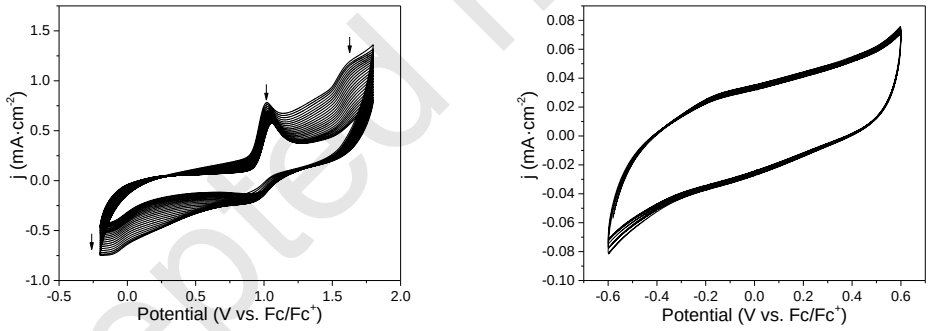

Fig. 3 Voltamperometric profiles of compound **3** (left) registered during electro-oxidation of the complex by 20 successive potentiodynamic scans under the working conditions detailed in Experimental; deposit response at the right (5 successive voltamperometric scans).

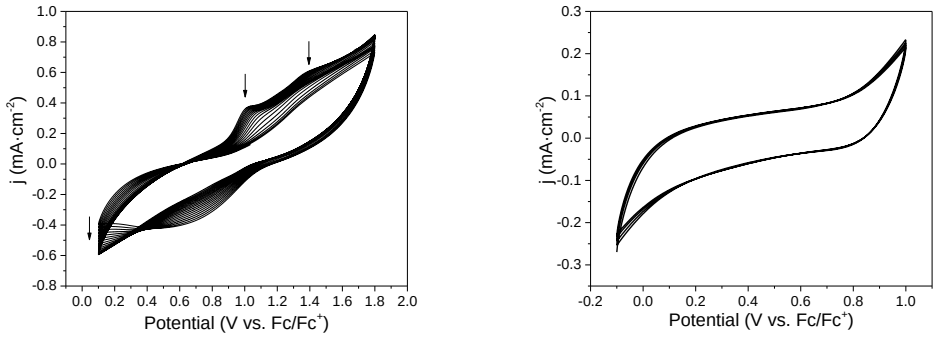

Fig. 4 Voltamperometric profile of compound **4** (left) registered during electro-oxidation of the complex by 20 successive potentiodynamic scans under the working conditions detailed in Experimental; deposit response at the right (5 successive voltamperometric scans).

After 20 cycles, the working electrodes were transferred to a solution containing only the supporting electrolyte in order to analyze its responses. As it is shown in the right part of Figs. 3 and 4, a *p*-doping/undoping process is observed, with current responses resembling that of analogous deposits prepared under similar conditions from complexes previously synthesized by us.[18,29,30] In any case, it should be noted that both deposits have a fully reversible charge response, as is the case with the other thiophene derivatives studied, they have been proposed to be tested as battery cathodes.[30,31] These results, which do not seem very auspicious in that sense, will allow to propose structural modifications in search of the preparation of metal containing polymers.

Theoretical investigations

DFT calculations were performed on compounds **1-4**, in order to shed some light on their electronic structure and understand their structure and properties. Details of the calculations are given in the Experimental section. Their fully optimized geometries are provided as xmol files in the ESI†. Consistently with the experimental observations (see above), the keto-enol and enaminone forms of **1** and **2** were found more stable than their alternative tautomers by 8.6 and 30.3 kcal·mol^{-1}, respectively. It is noteworthy that the free ligand **2** (Scheme 1) does not adopt a planar structure, but affords a rotation around the CH_2-CH_2 bridge in such a way the two *pseudo* 6-membered heterocycles are far from each other (see Fig. S5,

ESI†). The optimized structures of **3** and **4** are in a very good agreement with the experimental ones (see selected metrical data in Tables 2 and S1, ESI†). **3** and **4** are 16- and 17-electron square-planar transition-metal complexes, respectively. It follows that the ground-state of **3** is a singlet, whereas that of **4** is a doublet. The MO diagrams of **3** and **4** are shown in Fig. 5. Due to the spin-unrestricted nature of the calculations, each Kohn-Sham MO level in the diagram of **4** is split into two spinorbitals: one spin-up (left) and one spin-down (right). Considering first the closed-shell situation of **3**, its 3d atomic level generates in the complex a set of four non-bonding or weakly antibonding metal-based MOs which are occupied (Ni(II) = d^8) and a σ-antibonding d_{x2-y2} orbital which is vacant. The latter is the LUMO, whereas three among the former constitute the three highest occupied orbitals, the fourth one being the HOMO-5. The substantial computed HOMO-LUMO gap is consistent with the stability and diamagnetism of **3**. With one more electron, the d_{x2-y2}-based orbital of **4** is singly occupied, *i.e.* splits into one occupied and one unoccupied spinorbital. It should be noted that the 3d-type levels of **4** are lying far below the HOMO, a situation common for such Cu(II) square-planar species.[19,20]

Calculations on the oxidized forms of **3** and **4** were also performed to better understand their electrochemical behavior. The computed spin densities of $\mathbf{3}^{+/2+}$ and $\mathbf{4}^{2+}$ are shown in Fig. 6. $\mathbf{4}^{+}$ was found to be a closed shell isoelectronic to **3**. The shape of the $\mathbf{3}^{+}$ spin density indicates that the first oxidation occurs on the HOMO of **3** which has an important metal character. The ground state of $\mathbf{3}^{2+}$ was found to be a triplet, with the second oxidation involving the HOMO-2. However, substantial electron reorganization occurs upon oxidation, which relocates spin density on the ligands, with a significant participation of the thienyl moieties, in full agreement with the electrochemical data (see above). Similarly, the first oxidation of **4** occurs at the HOMO. The ground state of $\mathbf{4}^{2+}$ was found to be a doublet and resulting also from an important reorganization of the spin density on the thienyl groups.

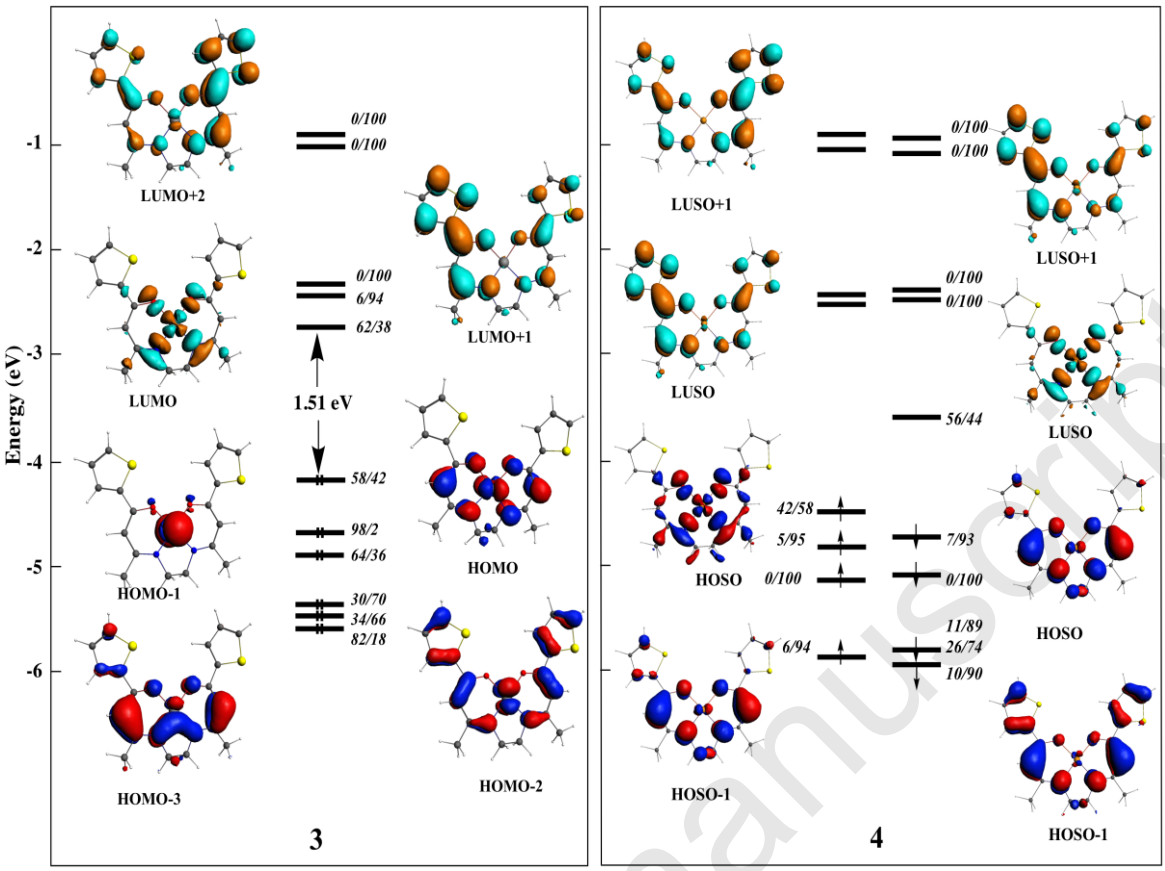

Fig. 5 Kohn-Sham orbital diagrams of **3** and **4**. The localizations (in %) are given in the following order: metal/ligand. HOSO: highest occupied spin-orbital; LUSO: lowest unoccupied spin-orbital.

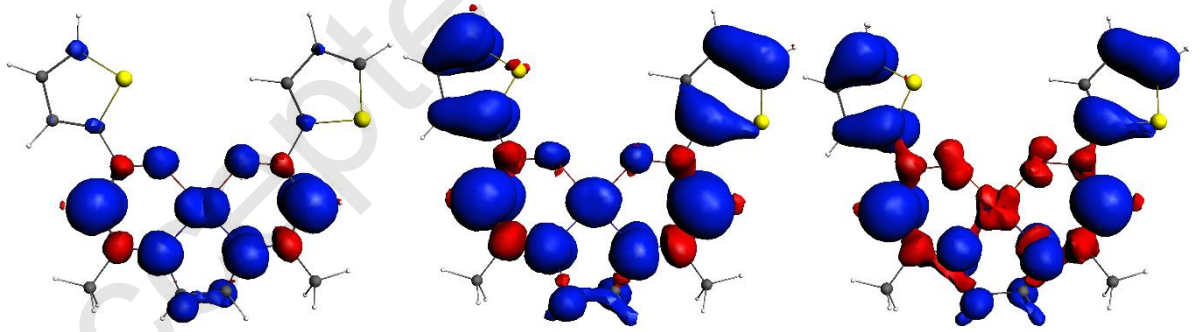

[3]$^{+}$ S=1/2 **[3]$^{2+}$ S=1** **[4]$^{2+}$ S=1/2**

Fig. 6 Computed spin densities of the ground states of **3**$^{+/2+}$ and **4**$^{2+}$.

TD-DFT calculations were performed on compounds **1**-**4** (see Table 1 and Fig. S8, ESI†) in order to index their optical transitions of low energy. As said above, the computed low-

energy transitions of **3** and **4** have different character, respectively of MLCT and LMCT nature. This difference comes from the fact that the d-type levels of **4** lie at much lower energy than those of **3** (see Figure 5).

Conclusions

In this contribution, two new Ni(II) and Cu(II) complexes featuring a symmetrically-substituted N_2O_2-tetradentate Schiff base ligand derived from the double condensation of 1-(2-thienyl)-1,3-butanedione with ethylenediamine, were prepared. The two organic species and the two coordination compounds were fully characterized by a variety of analytical and spectroscopic methods, as well as by X-ray crystallography for the nickel and copper complexes. 2D NMR experiments established that the Schiff condensation took place at the acetyl carbon of the diketone while geometry optimization depicted a non co-planarity of the two formed six-membered enaminone rings. Both the Ni(II) and Cu(II) metal ions adopt a perfect square planar geometry with partial delocalization of bonding electron density throughout the six membered heterometallacycle frameworks. Geometry, bonding, electronic structure and electrochemical properties have been rationalized by DFT calculations. Indexation of the optical transitions were supported by TD-DFT calculations. Cyclic voltammetry exhibits a similar potentiodynamic behavior for the Ni (II) and Cu (II) complexes with two oxidation processes occurring in each case. The first reversible event is associated to M(II)/M(III) redox couple while the second oxidation process is responsible for the formation of a low conductivity deposit of oligomeric units. Extension of the conjugation between the electroactive thienyl group and the metal core could facilitate the electrochemically-induced polymerization by the stabilization of the radical cation formed in the process, and also increase the conductivity of the final deposit. Work is currently being devoted toward this goal.

Experimental

Materials and physical measurements

Reactions were performed under dry dinitrogen or argon atmosphere using standard Schlenk techniques. Solvents were dried and distilled according to standard procedures.[32] All starting materials were purchased from commercial sources and used as received. Checking of

the purity of the organic compounds was carried out by TLC performed on silica coated Merck kieselgel 60F254 0.25 mm plates and visualized by UV irradiation at 254 nm. Solid-state FT-IR spectra were recorded on a Perkin-Elmer Model 1600 FT-IR spectrophotometer with KBr disks in the 4000 to 450 cm^{-1} range. Uv/Vis spectra were recorded using a Thermo Scientific, Helios Omega spectrophotometer. ^{1}H and ^{13}C NMR spectra were acquired at 298 K with a Bruker 300 FT-NMR spectrometer. Chemical shifts (δ) are reported in parts per million (ppm, δ), and referenced to the residual deuterated solvent peaks. Coupling constants (J) are reported in Hertz (Hz), and integrations are reported as the number of protons. ^{1}H and ^{13}C NMR chemical shift assignments are supported by data obtained from ^{1}H-^{1}H COSY and ^{1}H-^{13}C HSQC NMR experiments. High Resolution Electrospray Mass Spectra (HR-ESI-MS) were collected on a Bruker MAXI 4G spectrometer at the Centre Régional de Mesures Physiques de l'Ouest (CRMPO) at the Université de Rennes 1, France. Elemental analyses were conducted on a Thermo-Finnigan Flash EA 1112 CHNS/O analyzer by the Microanalytical Service of the CRMPO. Melting points were measured in evacuated capillaries on a Kofler Bristoline melting point apparatus and were not corrected.

Synthesis of 1-(2-thienyl)-1,3-butanedione (1)

A Schlenk tube was charged with a magnetic stirring bar, 1.00 g (7.93 mmol) of 2-acetyl thiophene and 30 mL of dry THF. The solution was stirred for 5 min. before adding 0.89 g (7.93 mmol) of *t*-BuOK, turning the solution from translucent to purple color. The reaction mixture was stirred for 45 min. Then, 1.94 mL (19.8 mmol) of ethyl acetate was added dropwise by syringe. After 30 min. of stirring, the volatiles were removed under vacuum, the solid residue was washed with 50 mL of an 1% aqueous HCl solution and extracted with diethyl ether (3 x 100 mL). The extracts were combined and evaporated to dryness. The solid material was absorbed on a column packed with silica gel (grade 60). Elution was carried out with hexane/ethyl acetate (24:1 v/v), and the collected colorless solution taken to dryness, affording 0.80 g of a white product. The white product was transferred into a new Schlenk tube along with 475 mg (2.38 mmol) of copper (II) acetate monohydrate and dissolved in 10 mL of methanol. The solution was stirred at 60 °C for 3 h. After cooling, 50 mL of an aqueous 1% HCl solution was added and the reaction mixture extracted with dichloromethane (3 x 100 mL). The extracts were combined, dried over anhydrous $MgSO_4$, filtered off and finally dried under vacuum, affording 0.73 g (4.34 mmol, 55% yield) of pure **1**. m.p. 51-52 °C (dec). Found: C, 57.07; H, 4.77; S, 18.93. *Calcd for* $C_8H_8O_2S$, requires: C, 57.12; H, 4.79; S, 19.06%. FT-IR (KBr, cm^{-1}): 3460(vs) ν(O-H); 3110(w), 3089(w) ν(C-H arom); 2969(vw), 2914(vw), ν(C-H

aliph); 1615 (vs), 1519 (m), 1413(m) ν(C···O) and ν(C···C); 722 (m) □(C-H SC_4H_3). ^{1}H NMR (300 MHz, $(CD_3)_2CO$): δ_H 2.11 (s, 3 H, CH_3), 6.29 (s, 1 H, CH=C), 7.21 (dd, $J_{H,H}$ = 4.9 and 3.8 Hz, 1 H, C_4H_3S), 7.86 (dd, $J_{H,H}$ = 4.4 and 1.4 Hz, 2 H, C_4H_3S), 15.80 (s, 1 H, O-H). $^{13}C\{^1H\}$ NMR (75.48 MHz, $(CD_3)_2CO$): δ_C 23.44 (*C*H_3), 96.87 (*C*H=C), 129.34 (C_4H_3S), 131.67 (C_4H_3S), 134.07 (C_4H_3S), 142.64 (C_{ipso}, C_4H_3S), 183.35 (CH=*C*), 187.92 (C=O).

Synthesis of the Schiff base proligand 2

A Schlenk tube was loaded with a magnetic stirring bar, 1.00 g (5.94 mmol) of **1** and 30 mL of dry ethanol. The solution was stirred for 5 min, and 0.20 mL (2.97 mmol) of 1,2-diaminoethane was added dropwise by syringe. The reaction mixture was stirred at r.t. for 18 h. The volatiles were evaporated and the solid residue dried under vacuum, providing 0.86 g (2.38 mmol, 80% yield) of a yellow powder. m.p. 73-74 °C (dec). found: C, 59.68; H, 5.66; N, 7.63; S, 17.50. Calcd for $C_{18}H_{20}N_2O_2S_2$, requires: C, 59.97; H, 5.59; N, 7.77; S, 17.79%. FT-IR (KBr, cm^{-1}): 3444 (w) ν(N-H); 3082 (vw), 3066(vw) ν(C-H arom); 2980(vw), 2940 (vw), 2876 (vw) ν(C-H aliph); 1595(vs), 1558(s), 1529(s) ν(C···O), ν(C···N) and/or ν(C···C); 705 (m) □(C-H C_4H_3S). ^{1}H NMR (300 MHz, $CDCl_3$): δ_H 2.03 (s, 6 H, CH_3), 3.51 (s, 4 H, CH_2), 5.56 (s, 2 H, CH=C), 7.04 (dd, $J_{H,H}$ = 4.9 and 3.7 Hz , 2 H, SC_4H_3), 7.43 (dd, $J_{H,H}$ = 4.9 and 1.1 Hz, 2 H, SC_4H_3), 7.51 (dd, $J_{H,H}$ = 3.7 and 1.1 Hz, 2 H, SC_4H_3), 11.17 (s, 2 H, N-H). $^{13}C\{^1H\}$ NMR (75.48 MHz, $CDCl_3$): δ_C 19.18 (CH_3), 43.81 (CH_2), 92.61 (-*C*H=C), 127.43 (C_4H_3S), 127.75 (C_4H_3S), 129.98 (C_4H_3S), 146.85 (C_{ipso}, C_4H_3S), 164.58 (C*H*=*C*), 181.28 (*C*=O).

Synthesis of the Ni(II) Schiff base complex 3

A Schlenk tube was charged with a magnetic stirring bar, 1.0 g (2.30 mmol) of **2,** 0.57 g (2.30 mmol) of nickel(II) acetate tetrahydrate and 15 mL of methanol. The reaction mixture was stirred for 4 h at r.t. Then, the resulting solution was evaporated under reduced pressure and the solid residue was washed with 100 mL of water and filtered off using a glass frit. The collected material was dissolved in CH_2Cl_2 and dried over $MgSO_4$. The suspension was filtered and evaporated under reduced pressure. The product was dried under vacuum, affording 0.81 g (1.93 mmol, 84% yield) of a light brown powder. Suitable single crystals for structure determination by X-ray diffraction were obtained by slow evaporation of an ethanolic solution of **3**. m.p. 288-289 °C. Found: C, 51.74; H, 4.37; N, 6.58; S, 15.01. Calcd for $C_{18}H_{18}N_2NiO_2S_2$, requires: C, 51.82; H, 4.35; N, 6.72; S, 15.37%. FT-IR (KBr, cm^{-1}): 3100 (w), 3070 (w) ν(C-H arom); 2990(w), 2941 (w), 2845 (w) ν(C-H aliph); 1581(s), 1530(s) and 1508(vs) ν(C···O),

□(C⋯N) and/or ν(C⋯C); 740 (m) □(C-H C_4H_3S). ^{1}H NMR (300 MHz, $CDCl_3$): δ_H 1.96 (s, 6 H, CH_3), 3.08 (s, 4 H, CH_2), 5.55 (s, 2 H, CH=C), 6.97 (m, 2 H, SC_4H_3), 7.30 (d, $J_{H,H}$ = 5.0 Hz, 2H, SC_4H_3), 7.38 (d, $J_{H,H}$ = 2.8 Hz, 2 H, SC_4H_3). ^{13}C{^{1}H} NMR (75.48 MHz, $CDCl_3$): δ_C 21.56 (*C*H_3) 53.32 (-*C*H_2), 96.56 (-*C*H=C), 125.51 (C_4H_3S), 127.35 (C_4H_3S), 127.81 (C_4H_3S), 143.24 (C_{ipso}, C_4H_3S), 165.16 (CH=*C*), 165.62 (*C*=O).

Synthesis of the Cu(II) Schiff base complex 4

Complex **4** was synthesized following an identical procedure to that described above for **3**, using in this case 0.46 g (2.30 mmol) of copper(II) acetate monohydrate. Yield: 0.87 g (2.07 mmol, 90%) of **4** as a green solid. Diffraction quality single crystals for structure determination were obtained by slow evaporation of an ethanolic solution. m.p. 209-210 °C. Found: C, 50.58; H, 4.47; N, 7.04; S, 14.79. Calcd for $C_{18}H_{18}CuN_2O_2S_2$, requires: C, 51.23; H, 4.30; N, 6.64; S, 15.20%. FT-IR (KBr, cm^{-1}): 3100 (w), 3080, 3070 (w) ν(C-H arom); 2993(w), 2938 (w), 2835 (w) ν(C-H aliph); 1588(s), 1527(vs) and 1506(s) ν(C⋯O), ν(C⋯N) and/or ν(C⋯C); 750 (m) □(C-H C_4H_3S). HRMS positive ESI, [m/z] calcd for [$C_{18}H_{18}N_2O_2S_2NaCu$]: 444.0003; found: 444.0001 $[M + Na]^+$.

X-ray crystal structure determination

A crystal of appropriate size and shape of each of the compounds **3** and **4** was mounted on top of a glass fiber in a random orientation. X-ray intensity data for both compounds were collected at 295(2) K on a D8 VENTURE Bruker AXS diffractometer equipped with a multilayer monochromated Mo-Kα radiation (λ = 0.71073 Å) and a CMOS Photon100 detector. The two structures were solved by dual-space algorithm using the SHELXT program,[33] and then refined with full-matrix least square methods based on F2 (SHELXL-2014).[34] The disorder observed for the carbon and sulfur atoms of the thiophene fragment in the two compounds was modelled using two positions per carbon and sulfur atom with refined occupancy factors of 0.65/0.35 and 0.75/0.25 in **3**, and 0.71/0.29 and 0.80/0.20 in **4**. For the two compounds, non-hydrogen atoms were refined with anisotropic displacement parameters. H atoms were included in their calculated positions, assigned fixed isotropic thermal parameters and constrained to ride on their parent atoms. A summary of the details about crystal data, collection parameters and refinement are documented in Table 3, and additional crystallographic details are in the CIF files. ORTEP views were drawn using *Olex2* software.[35]

Table 3. Crystallographic data, details of data collection and structure refinement parameters for compounds **3** and **4**.

	3	**4**
Empirical formula	$C_{18}H_{18}N_2NiO_2S_2$	$C_{18}H_{18}CuN_2O_2S_2$
Formula mass (g mol^{-1})	417.17	422.00
Collection T (K)	295(2)	295(2)
Crystal size (mm)	0.51 x 0.22 x 0.06	0.37 x 0.08 x 0.03
Crystal color	Brown	Orange
Crystal system	Monoclinic	Monoclinic
Space group	$P2_1/n$	$P2_1/n$
a (Å)	10.7771(7)	10.974(6)
b (Å)	8.1452(4)	8.129(3)
c (Å)	20.9571(12)	20.893(8)
ß (°)	99.414(2)	99.866(15)
V (Å^3)	1814.87(18)	1836.2(14)
Z	4	4
Dcalcd (g cm^{-3})	1.527	1.527
F(000)	864	868
Absorption coefficient (mm^{-1})	1.313	1.430
θ range (°)	3.151 to 27.437	3.135 to 27.483
Range h,k, l	-13/13, -9/10, -27/27	-14/14, -10/8, -26/22
No. independent refl.	14670	9473
No. unique refl. (>2)	4139	4036
Comp. to θ_{max} (%)	99.6	95.5
Max/min transmission	0.924/0.742	0.958 /0.573
Data/restraints/parameters	4139/0/230	4036/0/230
Final R indices [I>2σ(I)]	R_1 = 0.0564 wR_2 = 0.1470	R_1 = 0.1103 wR_2 = 0.2398
R indices (all data)	R_1 = 0.0871 wR_2 = 0.1728	R_1 = 0.2181 wR_2 = 0.2798
Goodness of fit/F^2	0.955	1.160
Largest diff. peak/hole (e A^{-3})	0.885/-0.722	0.602/-0.920

Electrochemical synthesis and characterization

Cyclic voltammetry (CV) measurements (electropolymerization and *in situ* characterization) were performed using a platinum disc working electrode ($7 \cdot 10^{-2}$ cm^2 geometric area), Ag|AgCl in tetramethylammonium chloride solution, to match the potential of a saturated calomel electrode (SCE) as reference, and a platinum wire of the large geometric area as auxiliary electrode, perturbing potentiodynamically (CV), by successive cycles at a potential scan rate of 100 mV·s^{-1}. The concentration of the complex under investigation was 10^{-3} mol·L^{-1} in acetonitrile solution containing 0.1 mol·L^{-1} supporting electrolyte. Ferrocene (Fc) was added as an internal reference at the end of each experiment. The Fc|Fc$^+$ couple was located at $E_{½}$ = 0.382 V *vs.* SCE in acetonitrile and at $E_{½}$ = 0.507 V *vs.* Cp*$_2$Fe$^{+/0}$ (Cp* =

C_5Me_5) which is independent of the solvent and supporting electrolyte,[36] where $E_{½}$ was calculated from the average of the oxidation and reduction peak potentials. Anhydrous acetonitrile (CH_3CN, 99.8%, Aldrich) stored over molecular sieves and tetrabutylammonium tetrafluoroborate (TBATFB, 99.0 % Aldrich) previously dried at 120 °C, were used as solvent and supporting electrolyte, respectively. All electrochemical measurements were accomplished on a CHI660E potentiostat at ambient temperature (20 °C) under high purity argon atmosphere, in a three-compartment, three-electrode anchor-type electrochemical cell. The response of the electrode after modification with the deposit produced by electro-oxidation of the metal complexes were studied in 10^{-1} mol·L^{-1} TBATFB in CH_3CN.

Computational details

DFT calculations were carried out for compounds **1**-**4** using the ADF2016 package,[37,38] employing the PW91 functional[39] and the TZ2P basis set.[40] Spin-unrestricted calculations were performed on the open-shell systems. The geometry optimizations in vacuum were carried out assuming the X-ray structures as input data, without any symmetry constraint. The optimized geometries were characterized as true minima on the potential energy surface using vibrational frequency calculations (no imaginary values). The UV-vis. transitions were calculated by means of TD-DFT calculations on the optimized geometries, at the same PW91/TZ2P level of theory.

Conflicts of Interest

The authors declare no conflict of interest.

Acknowledgments

We thank F. Lambert (CRMPO, Rennes) for helpful assistance with MS measurements. Financial support from the Fondo Nacional de Desarrollo Científico y Tecnológico [FONDECYT (Chile), grant no. 1140903 (C.M. and D.C.)], FONDEQUIP [EQM130154], the Vicerrectoría de Investigación y Estudios Avanzados, Pontificia Universidad Católica de Valparaíso, Chile (C.M. and D.C.), the CNRS and the Université de Rennes 1 is gratefully acknowledged. The GENCI-CINES and GENCI-IDRISS French national computer centers are acknowledged for computational resources (Grant a0010807367). This research has been

performed as part of the Chilean-French International Associated Laboratory “Multifunctional Molecules and Materials” (LIA M3 - CNRS N° 1207). G.A. and J.O. thank the CONICYT (Chile) for support of graduate fellowships N°21120098 and N°21171363, respectively.

References

1 A. Combes, *C. R. Acad. Sci.*, 1889, **108**, 1252-1255.

2 R. Hernandez-Molina and A. Mederos, *Acyclic and Macrocyclic Schiff Base Ligands*, Comprehensive Coordination Chemistry II, J. A. McCleverty and T. J. Meyer Eds., Elsevier Pergamon, Oxford, 2004, vol. 1, p. 411-458.

3 P. A. Vigato and S. Tamburini, *Coord. Chem. Rev.*, 2008, **252**, 1871-1995.

4 X. Liu, C. Manzur, N. Novoa, S. Celedón, D. Carrillo and J.-R. Hamon, *Coord. Chem. Rev.*, 2018, **357**, 144–172.

5 P.G. Cozzi, *Chem. Soc. Rev.*, 2004, **33**, 410-421.

6 J. Emsley, *Struct. Bonding*, 1984, **57**, 147-191.

7 S. Celedon, M. Fuentealba, T. Roisnel, J.-R. Hamon, D. Carrillo and C. Manzur, *Inorg. Chim. Acta*, 2012, **390**, 184-189.

8 S.S. Shapovalov, O.G. Tikhonova, A.V. Kolos, A.A. Pasynskii, I.V. Skabitsky, G.L. Denisov and V.A. Grinberg, *Polyhedron*, 2018, **149**, 73-78.

9 X. Shen, A. Jyoti Borah, X. Cao, W. Pan, G. Yan and X. Wu, *Tetrahedron Lett.*, 2015, **56**, 6484-6487.

10 I. Hussain, A. Riahi, M. A. Yawer, A. Villinger, C. Fischer, H. Gorls and P. Langer, *Org. Biomol. Chem.*, 2008, **6**, 3542-3551.

11 Y. Ba, B. V. Varun, K. Gadde and K. R. Prabhu, *Org. Lett.*, 2015, **17**, 2944-2947.

12 Y. Bai, W. Chen, Y. Chen, H. Huang, F. Xiao and G.-J. Deng, *RSC Adv.*, 2015, **5**, 8002-8005.

13 N. Novoa, T. Roisnel, V. Dorcet, J.-R. Hamon, D. Carrillo, C. Manzur, F. Robin-Le Guen and N. Cabon, *J. Organomet. Chem.*, 2014, **762**, 19-28.

14 G. Ahumada, T. Roisnel, S. Sinbandhit, C. Manzur, D. Carrillo and J.-R. Hamon, *J. Organomet. Chem.*, 2013, **737**, 1-6.

15 For a Progress Report, see: C. Friebe, M. D. Hager, A. Winter and U. S. Schubert, *Adv. Mater.*, 2012, **24**, 332–345, and references cited therein.

16 A. Zulauf, X. Hong, F. Brisset, E. Schulz and M. Mellah, *New J. Chem.*, 2012, **36**, 1399-1407.

17 A. Pietrangelo, B. N. Boden, M. J. MacLachlan and M. O. Wolf, *Can. J. Chem.*, 2009, **87**, 314-320.

18 J. Oyarce, L. Hernández, G. Ahumada, J. P. Soto, M. A. del Valle, V. Dorcet, D. Carrillo, J.-R. Hamon and C. Manzur, *Polyhedron*, 2017, **123**, 277-284.

19 G. Ahumada, M. Fuentealba, T. Roisnel, S. Kahlal, R. Córdova, D. Carrillo, J.-Y. Saillard, J.-R. Hamon and C. Manzur, *J. Mol. Struct.*, 2017, **1150**, 531-539.

20 G. Ahumada, M. Fuentealba, T. Roisnel, S. Kahlal, D. Carrillo, R. Cordova, J.-Y. Saillard, J.-R. Hamon and C. Manzur, *Polyhedron*, 2018, **151**, 279-286.

21 M. Fuentealba, J.-R. Hamon, D. Carrillo and C. Manzur, *New J. Chem.*, 2007, **31**, 1815-1825.

22 J. Cisterna, V. Artigas, M. Fuentealba, P. Hamon, C. Manzur, V. Dorcet, J.-R. Hamon and D. Carrillo, *Inorg. Chim. Acta*, 2017, **462**, 266-280.

23 P. Molina, A. Arques and I. Cartagena, *Thiophenes and their Benzo Derivatives: Structure*, *Comprehensive Heterocyclic Chemistry III*, A. R. Katritzky, C. A. Ramsden, E. F. V. Scriven and R. J. K. Taylor Eds., Elsevier, New York, 2008, Vol. 3, Chapter 09, p. 625-739.

24 A. M. Asiri, A. O. Al-Youbi, H. M. Faidallah and S. W. Ng, *Acta Crystallogr. Sect. E*, 2011, **67**, o2659-o2660.

25 R. D. G. Jones, *Acta Crystallogr. Sect. B*, 1976, **32**, 1224-1227.

26 L. Yang, D. R. Powell and R. P. Houser, *Dalton Trans.*, 2007, 955-964.

27 A. Trujillo, S. Sinbandhit, L. Toupet, D. Carrillo, C. Manzur and J.-R. Hamon, *J. Inorg. Organomet. Polym. Mater.*, 2008, **18**, 81-99.

28 A. Trujillo, F. Justaud, L. Toupet, O. Cador, D. Carrillo, C. Manzur and J.-R. Hamon, *New J. Chem.*, 2011, **35**, 2027-2036.

29 B. Gonzalez, M. A. del Valle, F. R. Diaz, C. Espinosa-Bustos, A. Ramirez and L. A. Hernandez, *Polyhedron*, 2015, **89**, 232-237.

30 B. Gonzalez, M. A. del Valle, F. R. Diaz, C. Espinosa-Bustos, A. Ramirez and L. A. Hernandez, *J. Appl. Polym. Sci.*, 2016, **133**, 43559-43565.

31 R. Gracia and D. Mecerreyes, *Polym. Chem.*, 2013, **4**, 2206-2214.

32 W. L. F. Armarego and C. L. L. Chai, *Purification of Laboratory Chemicals*, 5 ed., Butterworth-Heinemann, Elsevier Inc., Amsterdam, The Netherlands, 2003.

33 G. M. Sheldrick, *Acta Crystallogr.*, 2015, **A71**, 3-8.

34 G. M. Sheldrick, *Acta Crystallogr.*, 2015, **C71**, 3-8.

35 O. V. Dolomanov, L. J. Bourhis, R. J. Gildea, J. A. K. Howard and H. Puschmann, *J. Appl. Crystallogr.*, 2009, **42**, 339-341.

36 J. Aranzaes-Ruiz, M.-C. Daniel and D. Astruc, *Can. J. Chem.*, 2006, **84**, 288-299.

37 G. te Velde, F. M. Bickelhaupt, S. J. A. van Gisbergen, C. Fonseca Guerra, E. J. Baerends, J. G. Snijders and T. Ziegler, *J. Comput. Chem.*, 2001, **22**, 931-967.

38 ADF2013, SCM, Theoretical Chemistry, Vrije Universiteit, Amsterdam, The Netherlands, http://www.scm.com.

39 J. P. Perdew, K. Burke and Y. Wang, *Phys. Rev. B*, 1996, **54**, 16533-16539.

40 E. Van Lenthe and E. J. Baerends, *J. Comput. Chem.*, 2003, **24**, 1142-1156.